02,05

Effect of an Array of Submicron Magnetic Dots on Magnetization, Critical Current, and the Structure of Vortex Configurations in HTS

© A.N. Maksimova, I.A. Rudnev, I.A. Kashurnikov, A.N. Moroz

National Research Nuclear University „MEPhI“,
Moscow, Russia

E-mail: anmaksimova@mephi.ru

Received October 14, 2022
Revised February 2, 2023
Accepted February 3, 2023

A vortex lattice in a high-temperature superconductor (HTS) with an array of submicron magnetic dots on the surface has been studied by the Monte Carlo method within the framework of a three-dimensional model of a layered high-temperature superconductor. The adjustment of the vortex lattice to an array of magnetic points was observed — ordered states arising in the process of remagnetization — configurations of one, two, three, or more vortex filaments fixed to a single magnetic point. The occurrence of these configurations was accompanied by peaks on the magnetization curve. The influence of the HTS anisotropy on the adjustment of the vortex lattice is analyzed. The ordered configurations of the vortex lattice are also associated with the non-monotonic nature of the dependences of the superconductor critical current on the magnetic field. The influence of temperature, magnetic moment of points, and film thickness on the critical current is investigated. With an increase in temperature and a decrease in the magnetization of magnetic points, the maximum of the critical current shifts towards a lower field. The structure of vortex filaments in the inhomogeneous field of a magnetic point is analyzed in detail. The mechanism of the influence of ordered vortex configurations on magnetization and critical current is discussed.

Keywords: high-temperature superconductor, magnetization curve, Abrikosov vortices, current-voltage characteristic, ferromagnetic pinning centers, Monte Carlo method.

DOI: 10.21883/PSS.2023.04.55989.500

1. Introduction

Currently, artificial ferromagnetic–superconductor structures are of fundamental and application interest. It is a well-established experimental fact that the angular dependence of resistance of a superconducting film with a periodic array of magnetic dots on the magnetic film has sharp minima. These minima correspond to so-called matching field [1,2]. At the same time, some studies show the absence of such effects in the case of nonmagnetic impurities [3]. In [1] a rectangular array of submicron magnetic dots has been investigated (with a distance between dot centers of $1\,\mu$m). Depending on the magnitude of the magnetic field, the dots were magnetized up to the saturation or were in the state of magnetic vortex. The investigations were carried out for a thin film of Nb with permalloy dots applied on its surface. Pinning of vortices in the film is due to the scattering fields of the magnetic dots. The magnetic field in the experiment was oriented at an angle of 86° to the normal to the film plane; at the same time, it is well-established that Abrikosov vortices are caused by the field component perpendicular to the film. Dependencies of magnetic resistance on the magnetic field magnitude have shown the presence of hysteresis and minima related to the matching field. In [2] also a collective pinning of vortices has been observed on an array of magnetic dots and an emergence of field-induced superconductivity due to the scattering field of magnetic dots.

In [4] the effect of micron ferromagnetic dots as vortex pinning centers on the critical current of a $YBa_2Cu_3O_{7-x}$ thin film has been studied experimentally. Size of the dots was $3\,\mu$m, thickness of the superconductor layer was 250 nm, which was at the limit of modern technology. The magnetic moment of dots was oriented both in the layer plane and normal to it. It has been noted that almost two times increase of the critical current takes place in weak fields, and the experiment was showing that this increase was due to exactly the magnetic nature of pinning centers. Also, the remagnetization and the critical current of ferromagnetic–superconductor structures were investigated in [5], however, no critical current increase in weak magnetic fields has been found.

An attention is paid to the magnetic dots on the surface of superconducting film in theoretical works as well. In [6,7] the pinning of vortices on a magnetic dot has been studied in the London approximation. It has been shown that more than one vortices can be secured on a single magnetic dot. In [7] the demagnetization factor of dots has been taken into consideration, the force of pinning has been calculated and it has been shown that at a temperature of ~ 77 K (nitrogen boiling temperature) it is an order of magnitude higher than the force of pinning on intrinsic nonmagnetic defects. Vortex lattice near magnetic dots has been also investigated in [8–11].

A significant number of studies have been focused on the numerical solving of Ginzburg–Landau (GL) equations

for the hybrid ferromagnetic–superconductor structure, in particular, for the superconductor near the magnetic dot. In [12], by solving time GL equations, the dynamics of vortices has been investigated for a superconductor in a non-uniform field of magnetic dipole. In [13] the general case of a superconductor in an arbitrary external potential has been considered, vortex solutions has been found. In [14–17] different configurations of vortices and antivortices in hybrid ferromagnetic–superconductor structures has been derived, the possibility of existence of vortices containing several magnetic flux quanta has been shown.

Vortex lattice in a layered anisotropic high-temperature superconductor (HTS) is a complex system that demonstrate a large diversity of configurations in external field. Vortex line can be represented as a stack of flat layer vortices, the pancake vortices bound by an interplanar bond. In a tilted and non-uniform magnetic field tilted vortices, chains of Abrikosov vortices extended along the Josephson vortex, vortex molecules are observed. In some cases the arrangement of pancakes in a tilted vortex can result in an effective attraction of neighbor stacks of vortices [18–24]. In the general case, the problem of system of interacting vortices can not be solved analytically, therefore numerical methods become of major importance. The Monte Carlo method for a vortex system (pancakes are represented as an ensemble of classic interacting particles with a long-range potential) allows calculating magnetization curves, current-voltage curves (IU-curves), critical current of a layered anisotropic HTS with an arbitrary potential of pinning. In [6–12] special cases of isolated vortex or hexagonal vortex lattice have been analyzed, however, magnetization curves or critical current have not been calculated. The experimental determination of the effect of magnetic dot parameters on features of magnetization curves or magnetoresistance is related to the need to produce samples that are different in only one parameter and can be seriously challenging. Numerical solving of GL equations allows obtaining a vortex configuration typical for the given parameters of the magnetic dot and an arbitrary size of the system, however, in practice it can be achieved only for the sizes that are not more than a few times greater than the depth of magnetic field penetration into the superconductor. Therefore, the purpose of this study was to analyze by the Monte Carlo method the processes of remagnetization and transport current flow through a HTS-film with magnetic dots on the surface, to derive the dependencies of the critical current on the external magnetic field and temperature. For this purpose, in the three-dimensional model of layered HTS an approximated description of the interaction between a three-dimensional vortex line and a non-uniform field of magnetic dot is introduced.

2. Model description

The calculations were performed within a three-dimensional model of layered HTSC [25–30]. In this model a superconductor can be represented as a stack of superconducting CuO-planes separated by isolating gaps. The geometry of model is shown qualitatively in Fig. 1. The external magnetic field is directed along the axis of anisotropy (perpendicular to layers). The external field causes nucleation of Abrikosov vortices in the superconductor. Each Abrikosov vortex can be represented as a stack of flat layer vortices, pancakes bound by an interplanar bond. The interaction between pancakes in neighbor layers has an electromagnetic component and a Josephson component. The nucleation of vortex line is possible only at a boundary of the sample; under the effect of the Lorentz force from the Meissner current and the transport current the vortices pass into the depth of the superconductor. Vortices in Fig. 1 pass into the sample along the x axis, and along the y axis periodic boundary conditions are in force. Also, the Meissner current and the transport current are directed along the y axis.

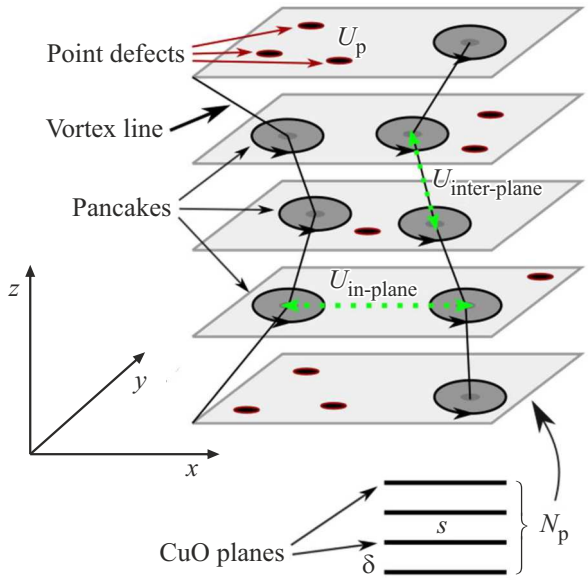

Figure 1. Geometry of the layered HTS model A general case of sample is shown that contains point defects of pinning.

Within this model, the energy of pancake system G is as follows:

$$G = \sum_z \Bigg\{ N_z \varepsilon + \sum_{i<j} U_{\text{in-plane}}(r_{ij}) + \sum_{i,j} U_p(r_{ij}) + \sum_{i,j} U_{\text{surf}}\left(r_{ij}^{(im)}\right) + \sum_i U_{\text{inter-plane}}\left(r_i^{z,z+1}\right) \Bigg\},$$

where $\varepsilon = d\varepsilon_0(\ln[\lambda(T)/\xi(T)] + 0.52)$ is intrinsic energy of vortex $\lambda(0)$, $\xi(0)$ is penetration depth and coherence length at$T = 0$; N_z is number of pancakes in the HTS-plane (ab) with a number of z; the second term describes the pairwise interaction of pancakes, the third term describes interaction of vortices with pinning centers, the fourth term describes interaction of vortices with the surface and the

Meissner current and the transport current, the last term describes interplanar interaction of pancakes;$\varepsilon_0 = \Phi_0^2/(4\pi\lambda)^2$, $\Phi_0 = \pi\hbar c/e$ is magnetic flux quantum. For a plate with a thickness of L_x the interaction between the vortex and the surface (the flat boundary) of superconductor is described as an interaction with its own specular reflection and reflections of other vortices. The energy of interaction with the Meissner current and the transport current is equal to the work of the Lorentz force when the vortex is moved from the plate edge to its location x, and has the following form:

$$U_{\mathrm{M}} = -\frac{1}{4\pi}\int\limits_{\pm L_x/2}^{x} j\Phi_0 dx$$

$$= d\,\frac{\Phi_0}{4\pi}\left(H_0\left(\frac{\mathrm{ch}\,\frac{x}{\lambda}}{\mathrm{ch}\,\frac{L_x}{2\lambda}} - 1\right) - H_I\left(\frac{\mathrm{sh}\,\frac{x}{\lambda}}{\mathrm{sh}\,\frac{L_x}{2\lambda}} \mp 1\right)\right),$$

$$j = -\frac{c}{4\pi\lambda}\left(H_0\,\frac{\mathrm{sh}\,\frac{x}{\lambda}}{\mathrm{sh}\,\frac{L_x}{2\lambda}} - H_I\,\frac{\mathrm{ch}\,\frac{x}{\lambda}}{\mathrm{ch}\,\frac{L_x}{2\lambda}}\right).$$

The external magnetic field $\mathbf{H}_0$ the field of current $\mathbf{H}_I$ are directed parallel to the axis of anisotropy (the c axis). The Meissner current and the transport current flow in the plane of HTS-layers (the ab plane). In the case of low anisotropy of the HTS, the relative displacement of pancakes in neighbor layers are small as compared to the average distance between vortex lines. Therefore, as it has been shown in [31], the energy of pairwise interaction of pancakes inside the Uin-plane is approximately proportional to $K_0(r/\lambda)$, K_0 is the Macdonald function.

For the interplanar interaction we used the shape of potential obtained in [31,32]:

$$U_{\text{inter-plane}}(r_i^{z,z+1}) = U_{\mathrm{em}}(r_i^{z,z+1}) + U_{\mathrm{Jos}}(r_i^{z,z+1}),$$

where U_{em} is electromagnetic interaction, U_{Jos} is Josephson interaction of pancakes located in neighbor layers. These terms are as follows:

$$U_{\mathrm{em}}(r_i^{z,z+1}) = 2d\varepsilon_0\left\lfloor C + \ln[r_i^{z,z+1}/(2\lambda)] + K_0(r_i^{z,z+1}/\lambda)\right\rfloor,$$

where $C = 0.5772$ is the Euler constant.

$$U_{\mathrm{Jos}}^{z,z+1}(r_i^{z,z+1}) =$$

$$= \begin{cases} \varepsilon_0 d\left[1+\ln\left(\frac{\lambda}{d}\right)\right] 0.25\left(\frac{r_i^{z,z+1}}{r_g}\right)^2 \ln\left(\frac{9r_g}{r_i^{z,z+1}}\right), & r_i^{z,z+1} \le 2r_g \\ \varepsilon_0 d\left[1+\ln\left(\frac{\lambda}{d}\right)\right]\left[\left(\frac{r_i^{z,z+1}}{r_g}\right) - 0.5\right], & r_i^{z,z+1} > 2r_g \end{cases},$$

where $r_g = \gamma d$ is typical distance of the Josephson interaction, γ is parameter of anisotropy, d is interplanar distance, $r_i^{z,z+1}$ is projection of the distance between pancakes located in z and $z+1$layers and belonging to the same vortex line on the ab plane.

Due to computer speed and memory limitations in the Monte Carlo calculation, it is possible to consider a stack of no more than 20 planes. At the same time, the minimum HTSC film thickness used in practice is about several hundreds of nm. The requirement of the aforementioned minimum film thickness is also related to the existence of a typical distance, at which the field of magnetic dot changes significantly in the experiment. This allows combining within our model a number of pancakes in neighbor planes and applying the sub-processes of nucleation, annihilation and movement to the stack of pancakes as a single object. This approach is possible because the real scale of the Abrikosov vortices bends is determined by the elastic parameters of the vortex line [33] and is usually much larger than the interlayer distance. In the following, a stack of $N_L = 100$ layer vortices is taken as a single object, thus, a system of 1200 CuO-layers is considered. This approach allows qualitatively reproducing main features of the vortex lattice in a weakly anisotropic superconductor, i.e. with $\gamma \approx 10$, and is limitedly applicable for strongly anisotropic HTSs. Therefore, in the following calculations $\gamma = 10$ is taken everywhere.

The magnetic moment of one dot is chosen as $\mu \approx 10^6\,\mu_{\mathrm{B}}$, where μ_{B} is the Bohr magneton. Such a magnetic moment corresponds to the dot size of 10–100 nm. The energy of interaction between a pancake and a magnetic dot on the surface of the HTS-layer depends on both the distance between centers of the dot and the pancake in the ab plane and the distance from the pancake to the surface in the direction of the axis of anisotropy. The energy of vortex in a superconducting film in the presence of a magnetic dipole above its surface has been calculated in the London approximation in [34]. By using the results of this study (for the dipole orientation perpendicular to the film plane) we combine approximately the energy for the cases of large and small distances between centers of the vortex and the dipole to derive an approximated representation for the pancake energy near the dot, which describes qualitatively the behavior of the interaction

$$U_{\mathrm{int1}} = \frac{U_{d0}}{\sqrt{2(r/\lambda)^2 + (l_d/\lambda)^2 + (r/\lambda)^6}},$$

where r is distance between centers of the pancake and the dot in the ab plane, l_d is some typical size. In these calculations we have chosen $l_d = \lambda$. U_{d0} is typical energy of pancake under the center of magnetic dot, its magnitude depends on μ and is chosen coincident in the order of magnitude with typical interaction energies of vortices. The case of vortex line near the magnetic dot is similar to the case non-uniform magnetic field that has been already considered by us [29]. The pancake energy decreases as $1/z^3$ with increase in the distance from the surface z, $z = ndN_L$. Thus, the final representation for U_{int1} is as follows:

$$U_{\mathrm{int1}} = \frac{1}{z^3}\,\frac{U_{d0}}{\sqrt{2(r/\lambda)^2 + (l_d/\lambda)^2 + (r/\lambda)^6}}.$$

It is worth to note that this representation does not take into account the screening of field in the direction

of c axis. However, the typical depth of magnetic field penetration in this direction is γ times greater than that in the plane of layers and, thus, it is comparable with the chosen film thickness. As can be seen from test calculations, vortex configurations do not change qualitatively with small quantitative variations of the potential.

The calculations are carried out for typical parameters of the $Bi_2Sr_2CaCu_2O_{8+\delta}$ bismuth-based HTS: $\lambda(T=0) = 180\,\text{nm}$, $\xi(T=0) = 2\,\text{nm}$, $T_c = 84\,\text{K}$, distance between HTS-layers is $s = 2.7\,\text{nm}$. This choice allows comparing the calculation results to the test calculations and results obtained by us earlier. The size of sample in the ab planes is $5 \times 3\,\mu\text{m}$. With the above-mentioned parameters, the typical energy of vortex line per one superconducting layer is 0.01–0.1 eV. The system has no nonmagnetic centers of pinning.

In this study magnetization curves and IU-curves of the superconductor with magnetic dots are calculated. The critical current has been determined from the IU-curve by the criterion of $1\,\mu\text{V/cm}$. Taking into account that in the resistive state the energy released on the sample per unit time is $Q = \delta d d_y j_s E$, where d is thickness of the sample, d_y is size in the direction of the transport current, j_s is average current density over the cross-section, the electric field strength E can be determined. The energy Q in the superconductor is equal to the energy released at annihilation of a vortex–antivortex pair in the center of the sample. If it is assumed that at each pair annihilation in the center a vortex and an antivortex are nucleated on opposite boundaries (which is really the case in the mode of running flow), then the energy released from the pair annihilation is equal to the work of Lorentz force when moving a vortex and an antivortex from sample edges to the center. The average current density is set as in input parameter for the calculation. This method of IU-curve calculation is developed in [26].

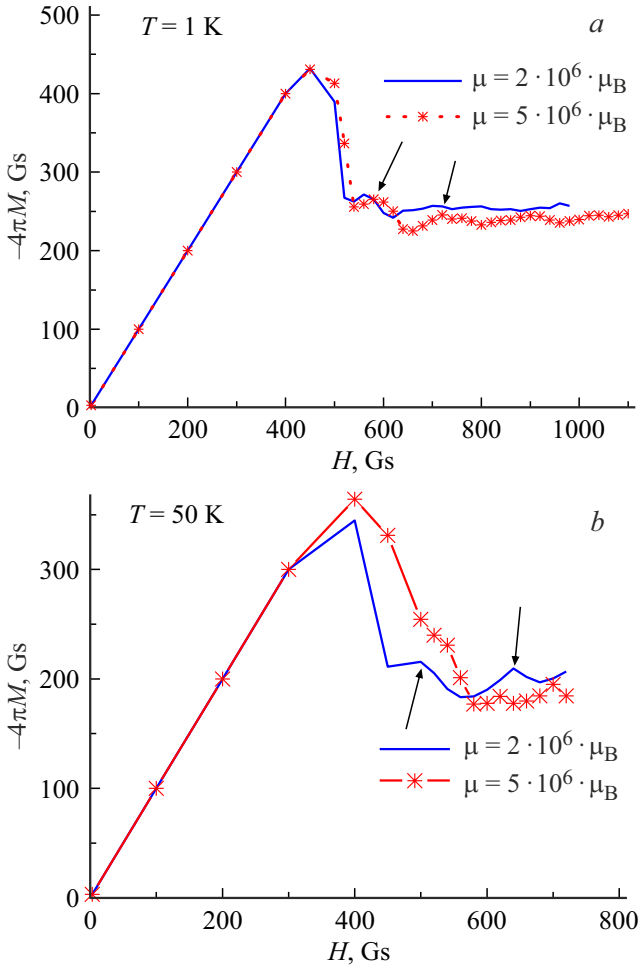

Figure 2. Magnetization curves of the film with magnetic dots at two values of magnetic moment of the dots. The film surface has 60 magnetic dots. $T = 1\,\text{K}$ (a), $T = 50\,\text{K}$ (b). Features in curves (shown with arrows) are related to effects of vortex lattice matching to the ordered lattice of magnetic dots.

3. Results

Let us analyze the process of remagnetization in a vortex system in the presence of magnetic dots with the above-listed parameters. The calculations will be performed for a HTS-plate with plane dimensions of ab $5000 \times 3000\,\text{nm}$. Let us assume that there are 60 magnetic dots on the sample surface, which is correspondent to the two-dimensional concentration of $4 \cdot 10^8\,\text{cm}^{-2}$ (according to preliminary calculations, such a concentration yields the most noticeable effects). Assume the magnetic moment of each dot is perpendicular to the plane of HTS-layers and has an order of magnitude of 10^6 Bohr magnetons.

Magnetization curves at two magnetic moments of the dot and at $T = 1\,\text{K}$ are shown in Fig. 1. In the calculations a fixed value of the anisotropy parameter of $\gamma = 10$ is taken. This value corresponds to the yttrium-based HTS, which is the most widely used in practical applications. According to preliminary calculations, with a low anisotropy the lattice matching effects are the most explicit. However, it is worth to note that all HTSs have different parameters of anisotropy; in particular, bismuth-based HTSs have $\gamma \approx 100$. It can be seen that the magnetization curve has features: more or less regular peaks, which are not smoothed with increase in temperature. These peaks can be considered as matching effects occurring in the vortex system, which are very similar to those that have been observed in many experiments with common nonmagnetic defects. The fact that peaks are kept at high temperature (over half of T_c) in Fig. 1, b may be related to rather high values of μ used in the calculations and the chosen value of γ. This phenomenon needs further investigation. It is worth to note some features (Fig. 2). The magnetic moment of dots probably determines the fields where the peaks occur: on both images they are slightly displaced to the right with increase in μ, which means that correspondent fields can be due to the magnetization of dots. Also, it is

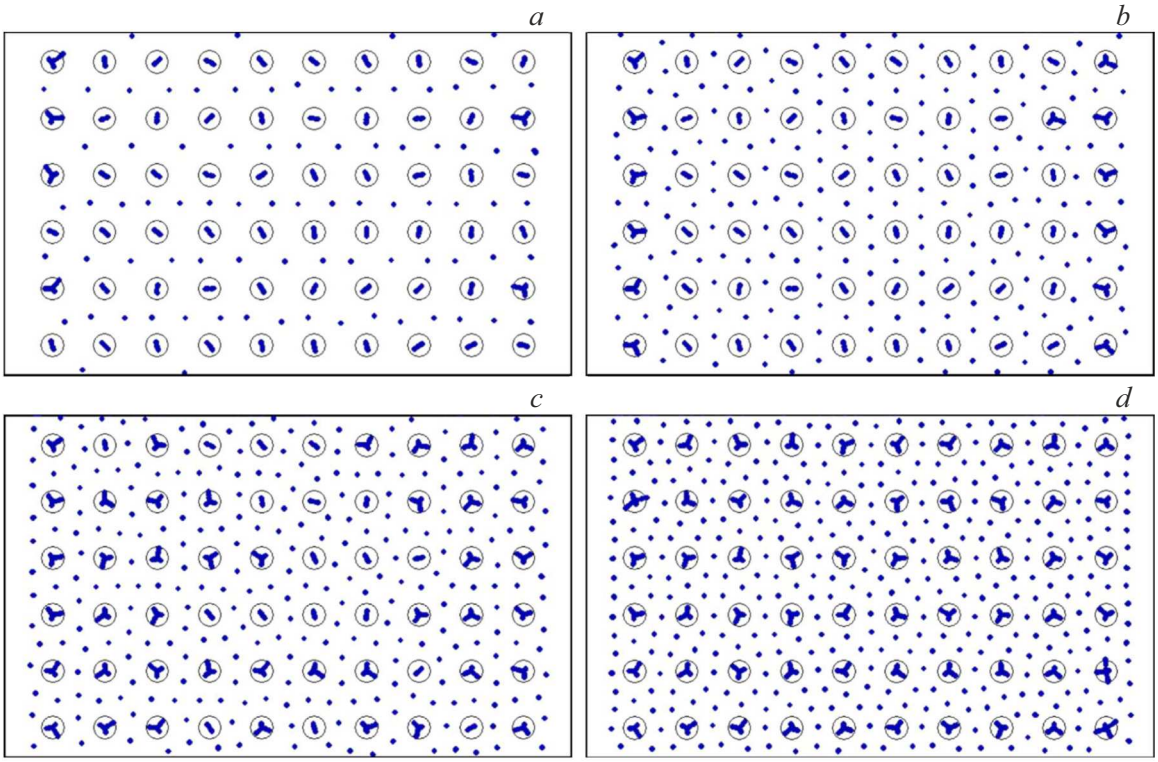

Figure 3. Ordered configurations of vortices resulting in features in the magnetization curve. Vortex configurations are shown in points of the curve corresponding to the following fields: *a* — 540, *b* — 660, *c* — 800, *d* — 960 Gs along the magnetization curve with $\mu = 5 \cdot 10^6 \cdot \mu_B$ in Fig. 2, *a*. Black circles show magnetic dots (their size is zoomed up for illustration purposes), blue circles correspond to pancakes.

worth to note that the difference between magnetization curves for two values of μ increases considerably with increase in temperature: despite the general lowering of the magnetization for both curves, the red curve is displaced up at $T = 50$ K in relation to the blue curve, and its decreasing slope becomes less rapid. Nonetheless, it can be seen that an increase in temperature also shifts the peaks to the left: for example, at $T = 1$ K the first noticeable peak of the blue curve is observed at approximately 580 Gs, and at 50 K the peak is observed near 500 Gs. In general, the above-mentioned features are indicative of the fact that the peaks really can be caused by appropriate effects in the vortex system because μ to some extent is an analog to the depth of quantum well of common nonmagnetic defects and changes in the magnetization curves caused by changes in μ and T are similar to those observed in the case of nonmagnetic defects.

The analysis of vortex configurations in points of the magnetization curve shows that the appearance of peaks is accompanied by ordered configurations of the vortex lattice (matching-effect). Such ordered configurations are related to the periodicity of the lattice of pinning centers and have been previously observed many times, including for nonmagnetic defects. Some of these configurations are shown in Fig. 3. Fig. 3 shows top view on the ab plane with individual pancakes shown with blue circles. Thus, a straight vortex line is represented in the figure as virtually a single circle, a tilted vortex line is shown as a stretched chain of circles. Fig. 4 shows the scheme of securing of several vortex lines on a magnetic dot. Due to the large depth of the quantum well under the dot center the pancakes in the top layer (the closest layer to the dot) are arranged very close to each other; inward the sample the attraction to the dot becomes weaker due to the mutual repulsion, and pancakes become away from each other at greater distances. This results in a tilt of the vortex line. It is worth to note that the higher is external magnetic field, the greater is number of vortices occupying magnetic dots: at 540 Gs (Fig. 4, *a*) there are two vortex lines per dot almost everywhere in the sample (except for some edge points occupied by three vortices), then in the range from 660 to 800 Gs (Fig. 4, *b* and *c*) more dots capture one additional vortex each and by 960 Gs (Fig. 4, *d*) each dot contains exactly three vortex lines. The vortex lines surrounding the occupied dots are straight and probably are distributed in a semi-ordered way in all figures. On other hand, all secured lines are tilted and go away from each other: the bigger is number of vortices in one dot, the bigger is the tilt angle.

In practice, the main goal of creation of magnetic defects in HTS films is the increase in critical current density j_c and the decrease in its dependence on the external magnetic field. Now let us consider the effect of the presence of

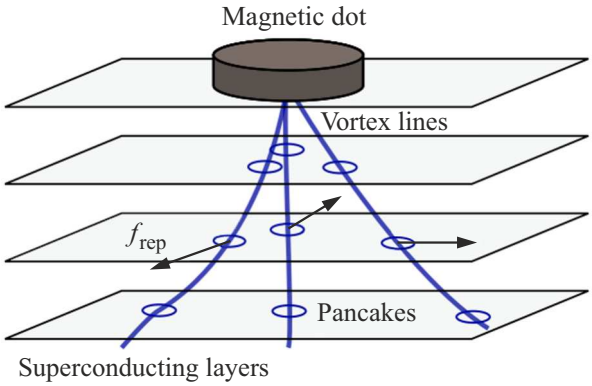

Figure 4. Scheme of arrangement of a number of vortex lines under a magnetic dot. Immediately under the dot the force of pancake attraction to it is sufficient to hold pancakes together, inward the film the force of the pairwise repulsion of vortices becomes prevailing over the attraction to the dot, which results in the above-mentioned arrangement of vortex lines.

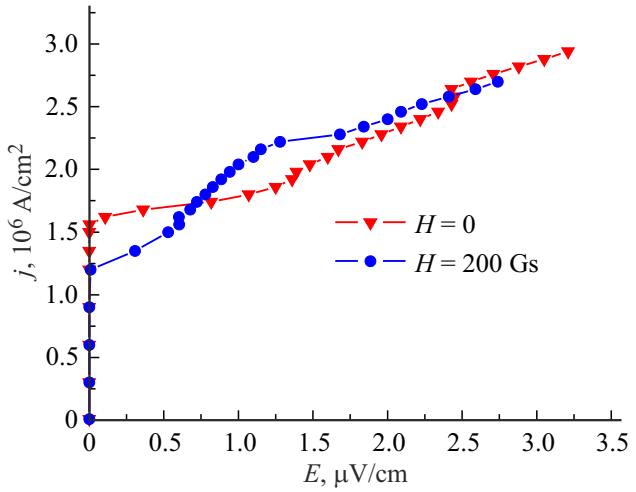

Figure 5. IU-curves calculated for a film with $\gamma = 10$ that contain 60 magnetic dots with $\mu = 5 \cdot 10^6\,\mu_B$ at 1 K in an external magnetic field of 200 Gs (blue circles) and in a zero external field (red triangles).

magnetic dots on j_c of our samples. This will be done by considering the calculated IU-curves. Fig. 5 shows two IU-curves (E is electric field generated inside the sample and j is current density) obtained for the same sample in its own current field and in an external magnetic field of 200 Gs. These curves were calculated for the sample that demonstrated the most explicit coinciding peaks in all our calculations. This sample corresponds to the red curve of magnetization in Fig. 2, *a*. Based on the IU-curve the j_c was determined by the standard criterion of 1 μV/cm at the given applied magnetic field. As can be seen from Fig. 5, shapes of IU-curves obtained at zero and non-zero external magnetic fields are significantly different: the curves have different slopes and are twisted in relation to each other (forming a 8-like shape before they start to be coincident at higher currents). These unique shapes occurred at different external magnetic fields in our calculations and probably were also caused by corresponding effects arising in the vortex system. The fact that the IU-curve shape changes when the external field is turned on suggests changes in the behavior of vortices motion through the sample as the external field grows. This issue will be considered and modes of the vortex flow manifested in this system will be thoroughly studied in our further research activities.

If the transport current flows through the sample in a zero magnetic field or in a field not greater than the field

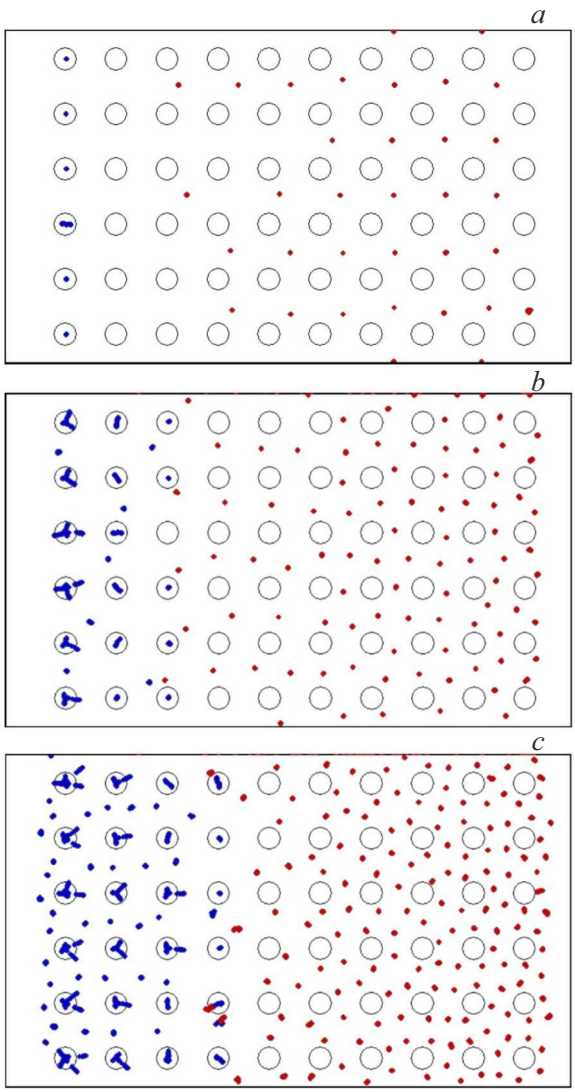

Figure 6. Vortex configurations arising during magnetization reversal by current. *a* — the current field at the plate edges is 450 Gs, which corresponds to an average current density of $1.35 \cdot 10^6$ A/cm^2; *b* — the current field at the plate edges is 580 Gs, the average current density is $1.74 \cdot 10^6$ A/cm^2; *c* — the current field at the plate edges is 800 Gs, the average current density is $2.4 \cdot 10^6$ A/cm^2. Vortices are shown with blue, antivortices are shown with red. Also, in the field of transport current matching effects are observed for vortices, which magnetic flux is parallel to magnetic moments of dots.

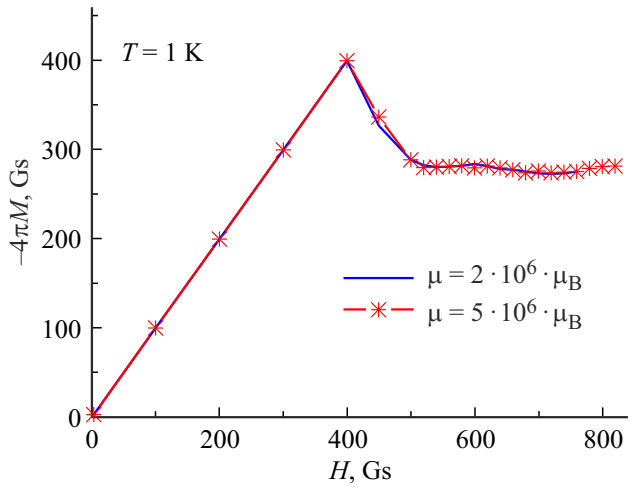

Figure 7. Magnetization curves at $T = 1$ K and two magnetic moments of dots (magnetic moments of dots are opposite to the magnetizing field). It can be seen that in this case the curves are merged.

of vortices entry, then vortices of different signs enter the sample from the left and the right boundaries. However, in our calculation for simplicity we assume that magnetic fields are magnetized to saturation and their magnetic moment is constant. Magnetic moments of all dots have the same direction. Thus, vortices with the sign opposite to the external field (antivortices) are repulsed from the magnetic dot. Vortex configurations for the IU-curve calculation are as follows (Fig. 6, calculation at $T = 1$ K for 60 magnetic dots and a magnetic moment of one dot of $5000\,\mu_B$).

It can be seen that vortices parallel to the external field are secured on magnetic dots and form ordered configurations on them, while antivortices are repulsed from the dots and in some cases form a regular lattice with alternating sites on magnetic dots and on antivortices. Such a behavior of antivortices is confirmed by the magnetization curve of superconductor in the case when magnetic moments of dots are opposite to the external field (Fig. 7). In contrast to curves shown in Fig. 2, *a*, curves in Fig. 7 are almost completely coincident and demonstrate no any visible peaks even at 1 K because dots in this case act as anti-securing sections and their magnetic moment has no effect on the shape of curves. The vortices secured on dots near the boundary screen the new vortices entering into the sample, which results in a critical current increase. It is worth noting that even in the absence of nonmagnetic defects the critical current of the film with magnetic dots in a number of cases is 10–20% higher than its typical values obtained by us with nonmagnetic defects [26,27]. One more feature which is worth noting is that although the IU-curve obtained at $H = 200$ Gs is the first that demonstrate non-zero electric field, it is the zero-field calculation curve that first crosses the criterion of $1\,\mu$V/cm, which results in a lower critical current. This may be a cause of ambiguity when determining $j_c(H)$ dependencies because the choice of criterion for the evaluation of j_c may lead to different results.

Let us investigate the effect of temperature on the density of critical current. Let us consider once again the $j_c(H)$ dependencies calculated for samples with 60 dots with various magnetization but at different temperatures from 1 to 50 K. The results are shown in Fig. 8: Fig. 8, *a* corresponds to $\mu = 5 \cdot 10^6\,\mu_B$ and Fig. 8, *b* corresponds to $\mu = 2 \cdot 10^6\,\mu_B$. There is a significant difference in general values of j_c between two images and between their behaviors with increase in H. The magnetic moment of dots equal to $5 \cdot 10^6\,\mu_B$ provides about 10–15% higher critical density of current than that of the sample in Fig. 8, *b* at any temperature under consideration. Moreover, its maximum j_c is achieved at slightly higher fields than those in the case of $\mu = 2 \cdot 10^6\,\mu_B$: no any visible maximum is seen in Fig. 8, *a* in fields below 700 Gs, while in Fig. 8, *b* j_c starts to decrease even at 600 Gs. An increase in temperature from 1 to 30 K does not result in any considerable changes in j_c in both samples and does not changes the general shape of its field dependence: wave-like behavior of the increasing tilt probable remains unchanged (for both values

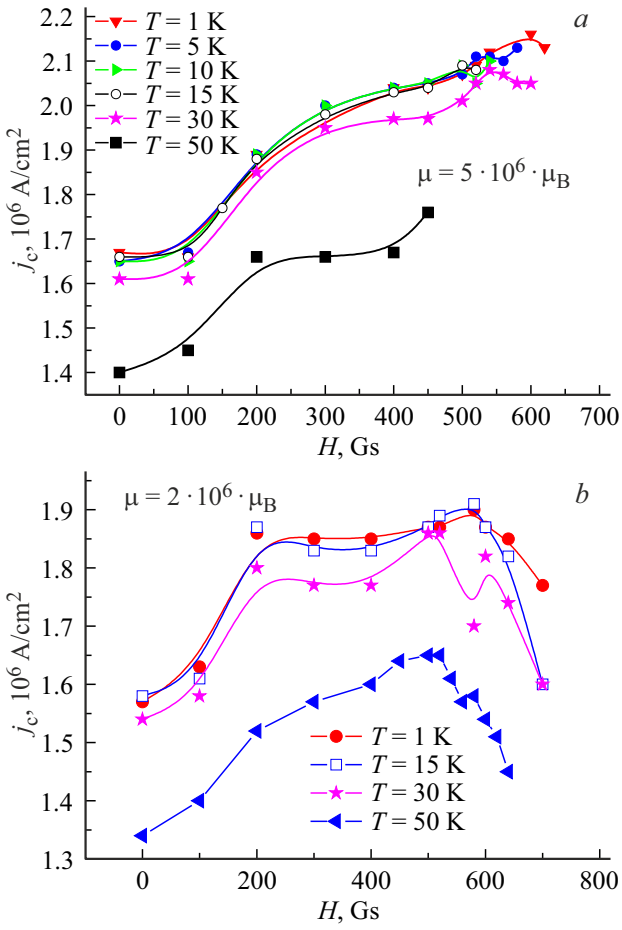

Figure 8. Dependence of critical current on magnetic field for the sample that contains 60 magnetic dots *a* — $\mu = 5 \cdot 10^6\,\mu_B$ and *b* — $\mu = 2 \cdot 10^6\,\mu_B$ at different temperatures.

of μ) and in Fig. 8, b field where critical density of current achieves its maximum is just slightly shifted to the left. At 50 K j_c decreases by approximately 10% in case of Fig. 8, a and slightly greater (about 12%) in Fig. 8, b but still demonstrates an increasing tilt with increase in H. In general, this parameter shows that the selected values of dot magnetization provide a good increase in j_c at temperatures up to at least 50 K. A decrease in the critical current after the maximum value is related to the fact that processes of penetration of new vortices into the sample start prevail over the screening by vortices secured on the dots. Due to a finite depth of dot potential the number of vortices that can be secured on it is limited.

Our results are qualitatively consistent with the experiment [4]. In [4] critical current of the film with magnetic dots is higher as compared to the current of the film without dots. At the same time, with increase in temperature increment in the critical current grows. In our calculations this can be referred to the more sharp tilt of the $j_c(H)$ dependence in Fig. 8, b at 50 K. It is worth to note that in [4] nonmonotonous dependencies of critical current have been observed for a sample with a hexagonal lattice of magnetic dots, for which the matching effects of vortex lattice are the most explicit.

Then, it is worth noting that in [4] the size of magnetic dot is a few μm with the distance between them of several tens of μm. In our calculations the dot size is several tens of nm with the distance between them equal to several hundreds of nm. Despite such a proportional increase in sizes results of the calculation and the experiment are qualitatively comparable. This suggests that vortex configurations obtained in the calculation correspond to those occurring in the experiment. Thus, the calculation allows identifying a transformation of vortex lattice in the presence of magnetic dots and the structure of vortex lines secured on the dots. Results of the calculation can be used to select the optimum configuration of magnetic dots in the experiment.

4. Conclusion

In the three-dimensional model of layered HTS a description of the interaction between the vortex line and the magnetic dot located on the surface of the HTS-film is introduced. Parameters used in the model correspond to the magnetic dot size of about several tens of nm and an average distance between dots from 100 to 200 nm.

The modeling of vortex lattice at different anisotropy of HTS has shown the presence of ordered vortex configurations near magnetic dots. Especially explicit is the ordering at a low anisotropy of $\gamma \approx 10$. In these configurations 1, 3 and more vortices are secured on one magnetic dot. Peaks in the magnetization curve are demonstrated, which are related exactly to these ordered configurations. Also, the IU-curves with differently sloped sections in magnetic field may be related to these configurations.

The effect of temperature, film thickness and dot magnetization on the critical current is analyzed. The following conclusions are made.

1. At any fields, the critical current is lower at a lower dot magnetization.

2. Dependencies of the critical current on the magnetic field have a growing behavior at low fields, which may be also related to the ordered vortex configurations.

3. With increase in temperature and decrease in dot magnetization maximum of the critical current shifts toward lower field.

Dependencies of the critical current on the magnetic field obtained in this study are qualitatively consistent with the experiment. Thus, it can be expected that vortex configurations obtained in this study also correspond to the vortex configurations that are realized in the experiment. The main result of this study is the identification of the behavior of vortex lattice transformation in the presence of magnetic dots, the demonstration of ordered vortex configurations and approximate mechanism of their impact on the magnetization and the critical current. Vortices secured on magnetic dots near the boundary of the sample screen new vortices in the sample. This mechanism results in both the formation of magnetization peaks and the growth of the critical current with increase in the magnetic field. This mechanism is effective at low magnetic fields.

Funding

The study was supported by the Russian Foundation for Basic Research within the research project No. 20-08-00811 (A.N. Maksimova, I.A. Rudnev), as well as supported by the Russian Foundation for Basic Research and „Rosatom“ State Corporation with the research project No. 20-21-00085 (V.A. Kashurnikov, A.N. Moroz).

Conflict of interest

The authors declare that they have no conflict of interest.

References

[1] A. Hoffmann, L. Fumagalli, N. Jahedi, J.C. Sautner, J.E. Pearson, G. Mihajlović, V. Metlushko. Phys. Rev. B **77**, *6*, 060506 (2008). https://doi.org/10.1103/PhysRevB.77.060506

[2] J.E. Villegas, K.D. Smith, L. Huang, Y. Zhu, R. Morales, I.K. Schuller. Phys. Rev. B **77**, *13*, 134510 (2008). https://doi.org/10.1103/PhysRevB.77.134510

[3] J.I. Martín, M. Vélez, J. Nogués, I.K. Schuller. Phys. Rev. Lett. **79**, *10*, 1929 (1997). https://doi.org/10.1103/PhysRevLett.79.1929

[4] M.M. Al-Qurainy, A. Jones, S. Rubanov, S.A. Fedoseev, I.A. Rudnev, A. Hamood, A.V. Pan. Supercond. Sci. Technol. **33**, *10*, 105006 (2020).

[5] I.A. Golovchanskiy, A.V. Pan, S.A. Fedoseev, M. Higgins. Appl. Surf. Sci. **311**, 549 (2014).

[6] R. Sasik, T. Hwa. (2000). arXiv preprint cond-mat/0003462
[7] W.J. Yeh, B. Cheng, T. Ragsdale. J. Modern Phys. **01**, *06*, 364 (2010). https://doi.org/10.4236/jmp.2010.16052
[8] K.Yu. Guslienko. Appl. Phys. Lett. **89**, *2*, 022510 (2006). https://doi.org/10.1063/1.2221904
[9] V.V. Moshchalkov, D.S. Golubović, M. Morelle. Comptes Rendus Phys. **7**, *1*, 86 (2006). https://doi.org/10.1016/j.crhy.2005.12.004
[10] A. Hoffmann, P. Prieto, V. Metlushko, I.K. Schuller. J. Supercond. Nov. Magn. **25**, *7*, 2187 (2012). https://doi.org/10.1007/s10948-012-1647-5
[11] J. del Valle, A. Gomez, E.M. Gonzalez, J.L. Vicent. (2016). arXiv preprint arXiv:1607.08416
[12] J. Wei, Y.J. Wu. Math. Phys. **62**, *4*, 041509 (2021). https://doi.org/10.1063/5.0028065
[13] B. Oripov, S.M. Anlage. Phys. Rev. E **101**, *3*, 033306 (2020). https://doi.org/10.1103/PhysRevE.101.033306
[14] M.V. Milošević, F.M. Peeters. Phys. Rev. B **68**, *2*, 024509 (2003). https://doi.org/10.1103/PhysRevB.68.024509
[15] B. Niedzielski, J. Berakdar. Phys. Status Solidi B **257**, *7*, 1900709 (2020). https://doi.org/10.1002/pssb.201900709
[16] R.M. Menezes, E. Sardella, L.R.E. Cabral, C.C. de Souza Silva. J. Phys.: Condens. Matter **31**, *17*, 175402 (2019). https://doi.org/10.1088/1361-648X/ab035a
[17] L. Peng, C. Cai, Y. Zhu, L. Sang. J. Low Temper. Phys. **197**, *5–6*, 402 (2019). https://doi.org/10.1007/s10909-019-02227-1
[18] A.E. Koshelev. Phys. Rev. B **71**, *17*, 174507 (2005). https://doi.org/10.1103/PhysRevB.71.174507
[19] A.E. Koshelev. Phys. Rev. B **48**, *2*, 1180 (1993). https://doi.org/10.1103/PhysRevB.48.1180
[20] A.E. Koshelev. Phys. Rev. Lett. **83**, *1*, 187 (1999). https://doi.org/10.1103/PhysRevLett.83.187
[21] A.E. Koshelev. Phys. Rev. B **68**, *9*, 094520 (2003). https://doi.org/10.1103/PhysRevB.68.094520
[22] A.V. Samokhvalov, A.S. Mel'nikov, A.I. Buzdin. Phys. Rev. B **85**, *18*, 184509 (2012). https://doi.org/10.1103/PhysRevB.85.184509
[23] J.R. Clem, M.W. Coffey. Phys. Rev. B **42**, *10*, 6209 (1990). https://doi.org/10.1103/PhysRevB.42.6209
[24] J.R. Clem, M.W. Coffey, Z. Hao. Phys. Rev. B **44**, *6*, 2732 (1991). https://doi.org/10.1103/PhysRevB.44.2732
[25] W. E. Lawrence, S. Doniach. Proceed. LT 12 Conf. Kyoto **1970**, 361 (1971).
[26] I.A. Rudnev, D.S. Odintsov, V.A. Kashurnikov. Phys. Lett. A **372**, *21*, 3934 (2008). https://doi.org/10.1016/j.physleta.2008.02.065
[27] V.A. Kashurnikov, A.N. Maksimova, I.A. Rudnev. Phys. Solid State **56**, *5*, 894 (2014). https://doi.org/10.1134/s1063783414050126
[28] V.A. Kashurnikov, A.N. Maksimova, I.A. Rudnev, D.S. Odintsov. J. Phys.: Conf. Ser. **1238**, *1*, 012016 (2019). https://doi.org/10.1088/1742-6596/1238/1/012016
[29] A.N. Maksimova, V.A. Kashurnikov, A.N. Moroz, I.A. Rudnev. Phys. Solid State **63**, *5*, 728 (2021). https://doi.org/10.1134/S1063783421050115
[30] V.A. Kashurnikov, A.N. Maksimova, I.A. Rudnev, D.S. Odintsov. J. Siberian Federal University. Math. Phys. **11**, *2*, 227 (2018). https://doi.org/10.17516/1997-1397-2018-11-2-227-230
[31] S. Tyagi, Y.Y. Goldschmidt. Phys. Rev. B **70**, *2*, 024501 (2004). https://doi.org/10.1103/PhysRevB.70.024501
[32] Y.Y. Goldschmidt, S. Tyagi. Phys. Rev. B **71**, *1*, 014503 (2005). https://doi.org/10.1103/PhysRevB.71.014503
[33] G. Blatter, M.V. Feigel'man, V.B. Geshkenbein, A.I. Larkin, V.M. Vinokur. Rev. Modern Phys. **66**, *4*, 1125 (1994). https://doi.org/10.1103/RevModPhys.66.1125
[34] M.V. Milošević, S.V. Yampolskii, F.M. Peeters. Phys. Rev. B **66**, *17*, 174519 (2002). https://doi.org/10.1103/PhysRevB.66.174519

Translated by Y.Alekseev